Proceedings of the 10th Brazilian Congress of Thermal Sciences and Engineering – ENCIT 2004
Braz. Soc. of Mechanical Sciences and Engineering – ABCM, Rio de Janeiro, Brazil, Nov. 29 – Dec. 03, 2004

Paper CIT04-0834

SOME CONSEQUENCES OF MATERIAL FRAME-INDIFFERENCE ON THE CALCULATION OF FLOW PAST A CIRCULAR CYLINDER

G. MOMPEAN, L. THAIS and L. HELIN
Laboratoire de Mécanique de Lille, LML UMR CNRS 8107, Ecole Polytechnique Universitaire de Lille, USTL, Cité Scientifique, 59655 Villeneuve d'Ascq, France
gilmar.mompean@eudil.fr

Abstract. *The purpose of the present study is to assess the importance of Material-Frame-Invariance (MFI) when modeling practical fluid flows. The MFI is a fundamental principle of continuum mechanics and an important and controversial topic when applied to derive constitutive laws for turbulent Newtonian flows and viscoelastic liquids. The results of direct numerical simulations of the Navier-Stokes equations for the two-dimensional flow past a circular cylinder are used to illustrate and to support this study. The angular velocity of the principal directions of the rate-of-deformation tensor are calculated in order to obtain an Euclidean objective vorticity tensor. This has direct consequences on the numerical simulations for various industrial fields (aeronautics, automotive, polymer processing, etc.). From the point of view of an engineer, the paper raises questions concerning the flow regions where the MFI should be taken into account or reasonably neglected.*

keywords: *Material frame-indifference, Euclidean objectivity, Algebraic stress models*

1. Introduction

Laminar flows of viscoelastic liquids and turbulent flows of Newtonian fluids carry widespread scientific and industrial interest due to their numerous applications in aeronautics, environment, automotive, polymer processing, paints, food, etc. In the process of deriving constitutive laws to predict such complex flows, the principle of material frame-indifference, hereafter named 'MFI', is said to play an important role (Truesdell and Noll, 1965). MFI is a general purpose principle emerging from continuum mechanics. This principle stems from the indifference of material properties to its observation : two observers in different reference frames should see the same material properties of a continuous media. The role and implications of MFI remain to date controversial in continuum mechanics (Liu, 2004 ; Murdoch, 2003). It also appears to be closely related to the mathematical property of Euclidean objectivity.

1.1. Euclidean objectivity

Euclidean objectivity was the cornerstone of the rheological theory of Oldroyd, 1950, who introduced the Euclidean objective Oldroyd derivative in his differential model of viscoelastic stresses (see also Joseph, 1990, page 7). Euclidean objectivity is a property regarding the transformation behavior of a tensor $\mathbf{T}$. Considering two different observers related by a time-dependent rigid transformation (rotation or translation of the reference frame known as a Euclidean transformation), a second-order tensor $\mathbf{T}$ will be qualified as Euclidean objective if

$$\mathbf{T}^* = \mathbf{Q}\,\mathbf{T}\,\mathbf{Q}^T. \tag{1}$$

In Eq. (1), $\mathbf{T}$ is the tensor given in a reference frame $\mathcal{R}$, $\mathbf{T}^*$ is the same tensor expressed in a new frame $\mathcal{R}^*$, and $\mathbf{Q}(t)$ the time-dependent matrix representing the rigid rotation from $\mathcal{R}$ to $\mathcal{R}^*$. It is well known that the rate-of-deformation tensor

$$\mathbf{S} = \frac{1}{2}\left(\nabla\mathbf{v} + \nabla\mathbf{v}^T\right) \tag{2}$$

is Euclidean objective, whereas the vorticity tensor

$$\mathbf{W} = \frac{1}{2}\left(\nabla\mathbf{v} - \nabla\mathbf{v}^T\right) \tag{3}$$

which measures the rate of rotation with respect to an arbitrary reference frame, is not Euclidean objective. In these equations, the velocity gradient is defined as $(\nabla\mathbf{v})_{ij} = \partial v_j/\partial x_i$, and $\nabla\mathbf{v}^T$ is its transpose.

1.2. Principle of material frame-indifference

The principle of MFI states that constitutive laws of an Euclidean objective quantity should be independent of observers. Physically, this means that different observers will see the same material property. Mathematically, this can be expressed as follows. Given $\mathbf{T} = F(\mathbf{X}_i)$ in the reference frame $\mathcal{R}$, and $\mathbf{T}^* = F^*(\mathbf{X}_i^*)$ in the reference frame $\mathcal{R}^*$, where $(\mathbf{X}_i, \mathbf{X}_i^*)_{i=1,n}$ are some properties in the respective frames, then we must have $F^* = F$, i.e. the constitutive functions are form-invariant under any Euclidean transformation. Combining the definition of objectivity equation (1) with the requirement of MFI, provides the following relationship

$$F(\mathbf{X}_i^*) \;=\; \mathbf{Q}\, F(\mathbf{X}_i)\, \mathbf{Q}^T. \tag{4}$$

This relationship is called the condition of material objectivity (see Liu, 2004). It is also sometimes named in short 'objectivity' in the literature. An interesting consequence of Eq. (4) is that if one of the arguments $\mathbf{X}_i$ is a non-objective quantity, then the constitutive model will not satisfy MFI, nor will it be Euclidean objective. We provide such an example in section 4.

The independence of objectivity and MFI has been disputed in a recent paper by Murdoch, 2003, in which it is claimed that MFI is a consequence of Euclidean objectivity. Yet, it is widely admitted in the literature that these notions are distinct. Liu, 2004 provides examples for which constitutive functions of elastic solids can be Euclidean objective without satisfying MFI. Another known example is three-dimensional (3-D) turbulence[1]. Speziale, 1998 showed that the modeled Reynolds stress equations do not satisfy MFI, although they are Euclidean objective. More generally, Speziale, 1998 established the exact circumstances under which the flow dynamics should give rise to constitutive laws which satisfy the principle of MFI : he proved that MFI should hold whenever there is a clear separation of time scales between the mean and fluctuating motions. This does not hold for 3-D turbulence, but does apply to two-dimensional (2-D) turbulence. A practical implication of this important result is that turbulence models when applied in the 2-D limit should satisfy MFI. Ristorcelli et al., 1995 proposed a turbulence model exhibiting this property.

1.3. Material frame-indifference in the context of explicit algebraic stress models

Another interesting result in Speziale, 1998 is that any constitutive equation with explicit dependence of the vorticity will never satisfy the principle of MFI, eventhough this equation can be Euclidean objective. This result, which was established in the framework of second-order closures for turbulence based on the Reynolds stress transport equations, appears to hold for the development of explicit algebraic stress models. Such models are derived through reduction of constitutive differential equations, for instance Oldroyd-B for viscoelastic fluids and Reynolds stress transport equations for turbulent flows. The reduction of the differential equations is usually based on an equilibrium hypothesis in the form $\mathrm{D}\mathbf{b}/\mathrm{D}t \simeq \mathbf{0}$, applied to a traceless tensor $\mathbf{b}$, (see Mompean et al., 1998). Algebraic models based on this hypothesis are non-objective. A closer analysis shows that frame-dependence enters *implicitly* in such models through the occurrence of the non-objective material derivative $\mathrm{D}/\mathrm{D}t$ in the equilibrium assumption. As a consequence, these models can be closed with a polynomial dependence in the form

$$\boldsymbol{\tau} = \boldsymbol{\tau}(\mathbf{S}, \mathbf{W}, \{\boldsymbol{\tau}\}), \tag{5}$$

where $\boldsymbol{\tau}$ is the stress tensor, and $\{.\}$ represents the trace operator.

The exact mathematical expression of the dependence in the above equation is not needed for the present discussion. The important point here is that frame-dependence enters *explicitly* in Eq. (5) due to the occurrence of vorticity, which is non-objective. Any such explicit stress function cannot satisfy the principle of MFI as expressed in Eq. 4. The non-objectivity of tensor $\mathbf{W}$ was discussed by Drouot, 1976, who also proposed a new Euclidean objective vorticity tensor. In this paper, a new kinematic tensor $\boldsymbol{\Omega}$ was defined as the rate of rotation of tensor $\mathbf{S}$ at a particle, or equivalently the rate of rotation of the principal directions of $\mathbf{S}$. Mathematically, the angular velocity tensor $\boldsymbol{\Omega}$ is given by

$$\frac{\mathrm{D}\,\mathbf{e}_i}{\mathrm{D}t} = \boldsymbol{\Omega}\,.\,\mathbf{e}_i, \tag{6}$$

where $\mathrm{D}/\mathrm{D}t$ is the material time derivative and $\mathbf{e}_i$ the unit eigenvectors of $\mathbf{S}$. Drouot, 1976 then introduced the Euclidean objective rate of rotation defined as the difference

$$\overline{\mathbf{W}} = \mathbf{W} - \boldsymbol{\Omega}. \tag{7}$$

[1] In fluid mechanics, the kinetic theory of gases was the first to be shown not to satisfy MFI.

Physically, this new tensor $\overline{\mathbf{W}}$ measures the rate of rotation of a particle with respect to the direction of maximum stretch at that particle. It can be formally shown that, although $\mathbf{W}$ and $\mathbf{\Omega}$ are frame-dependent, their difference $\overline{\mathbf{W}}$ is Euclidean objective.

In recent studies, an improved procedure involving the Euclidean objective vorticity $\overline{\mathbf{W}}$ was proposed to get general algebraic Euclidean objective stress expressions. Rumsey et al., 2000 applied this procedure in the context of turbulence closure, whereas Mompean et al., 2003 applied a similar technique for extra-stresses in viscoelastic liquids. These new models are based on a general Euclidean objective equilibrium hypothesis in the form $\mathcal{D}\mathbf{b}/\mathcal{D}t \simeq \mathbf{0}$, where $\mathcal{D}/\mathcal{D}t$ is an Euclidean objective derivative. Mompean et al., 2003 also showed how a suitable choice for the Euclidean objective derivative $\mathcal{D}/\mathcal{D}t$ (Jaumann or Harnoy derivative, or any weighted average of these) allowed prediction of a non-zero second normal stress difference, a feature that both the differential Oldroyd-B model and the frame-dependent algebraic model of Mompean et al., 1998 would fail to provide. With this Euclidean objective equilibrium assumption, a new polynomial expansion for the stresses is

$$\boldsymbol{\tau} = \boldsymbol{\tau}(\mathbf{S}, \overline{\mathbf{W}}, \{\boldsymbol{\tau}\}), \tag{8}$$

where the functional dependence now includes the Euclidean objective vorticity (see Eq. 7).

From this brief review, it appears that the principle of MFI has wide applications in fluid mechanics. Yet, truly frame-independent stress models remain scarce in the literature. Also, the circumstances under which MFI should be taken into account in practical engineering flows remain unclear. We propose in this paper to use the Euclidean objective rate of rotation $\overline{\mathbf{W}}$, i.e. the difference between the vorticity tensors $\mathbf{W}$ and $\mathbf{\Omega}$, as a measure of the influence of MFI. To achieve this goal, results from numerical simulations of the Navier-Stokes equations will be considered for the 2D-flow past a circular cylinder.

The paper is organized as follows. In section 2, we provide the methodology for computing and analyzing fields of angular velocity $\mathbf{\Omega}$ for complex flows. In section 3, this methodology is applied to the flow past a circular cylinder. In section 4, the consequences of MFI upon algebraic extra-stress models for viscoelastic fluids are examined. Finally, the results are discussed in section 5.

2. Evaluation of the Euclidean objective vorticity tensor

In this section, we provide the methodology for evaluating and analyzing fields of the angular velocity $\mathbf{\Omega}$ (the rate of rotation of tensor $\mathbf{S}$). The discussion starts with simple flows for which the interpretation of the principal directions of $\mathbf{S}$, as well as its rotation velocity, are straightforward. We shall consider the case of uniform extension, uniform shear, and non-uniform shear (Couette flow). The results for these simple flows will be used to help in the interpretation of complex flows. Finally, a general method for computing $\mathbf{\Omega}$ in complex two-dimensional flows is presented.

2.1. Flow classifier

In order to locally identify the nature of the flow kinematics, a general purpose flow classifier is needed. In this study the flow classifier proposed by Astarita, 1979 will be used. Astarita's criterion is based on the dimensionless parameter R defined as

$$R = -\frac{\{\overline{\mathbf{W}}^2\}}{\{\mathbf{S}^2\}}, \tag{9}$$

with $\{.\}$ representing the trace operator. This parameter is a measure of how much the material avoids stretching through rotation relative to the principal directions of $\mathbf{S}$. Following Mompean et al., 2003, this parameter is re-normalized as

$$D = \frac{1-R}{1+R}. \tag{10}$$

The parameter D is bounded between -1 and +1, which avoids numerical problems whenever R gets large. Its limiting values in the considered flows are discussed in the next subsection.

2.2. Extensional, shear and Couette flows

2.2.1. Uniform extensional flow

For a uniform planar extensional flow the rate-of-deformation tensor and the vorticity tensor are

$$\mathbf{S} = \begin{bmatrix} \dot{\epsilon} & 0 \\ 0 & -\dot{\epsilon} \end{bmatrix}, \quad \mathbf{W} = \begin{bmatrix} 0 & 0 \\ 0 & 0 \end{bmatrix} \tag{11}$$

with $\dot{\epsilon}$ the uniform elongation rate independent of the space coordinates. For $\dot{\epsilon} > 0$ (extensional flow), the eigenvectors are $\mathbf{e_1} = (-1, 0)^T$ and $\mathbf{e_2} = (0, -1)^T$, with $\mathbf{e_1}$ related to the first eigenvalue $+\dot{\epsilon}$, and $\mathbf{e_2}$ related to the second eigenvalue $-\dot{\epsilon}$. The angle ϕ between the second eigenvector and the inertial Cartesian basis is $-\pi/2$. For $\dot{\epsilon} < 0$, the eigenvectors are $\mathbf{e_1} = (0, -1)^T$ and $\mathbf{e_2} = (1, 0)^T$. The angle ϕ between the second eigenvector and the inertial Cartesian basis is $\phi = 0$.

In flow regions characterized by uniform (space-independent) elongation, the principal direction ϕ is fixed with respect to any inertial reference frame, which implies that the angular velocity $\mathbf{\Omega}$ in such regions will be zero. Therefore, for uniform elongation flows, $\{\overline{\mathbf{W}}^2\} = \{\mathbf{W}^2\} = 0$, which implies $R = 0$, and hence $D = +1$ (see Eq. 9 and 10) .

2.2.2. Uniform shear flow

For a two-dimensional uniform shear flow the rate-of-deformation tensor and the vorticity tensor are

$$\mathbf{S} = \begin{bmatrix} 0 & \dot{\gamma} \\ \dot{\gamma} & 0 \end{bmatrix}, \quad \mathbf{W} = \begin{bmatrix} 0 & -\dot{\gamma} \\ \dot{\gamma} & 0 \end{bmatrix} \tag{12}$$

where $\dot{\gamma}$ is the uniform (space-independent) shear rate. In this case, the eigenvectors are $\mathbf{e_1} = (-1, -1)^T$ and $\mathbf{e_2} = (1, -1)^T$, with $\mathbf{e_1}$ related to the first eigenvalue $+\dot{\gamma}$, and $\mathbf{e_2}$ related to the second eigenvalue $-\dot{\gamma}$. The angle ϕ between the second eigenvector and the inertial Cartesian basis is $-\pi/4$.

In flow regions characterized by uniform (space-independent) shear, the principal direction ϕ is again fixed with respect to any inertial reference frame, which implies that the angular velocity $\mathbf{\Omega}$ in such regions will also be zero. For uniform shear flow, $\{\overline{\mathbf{W}}^2\} = \{\mathbf{W}^2\} = -2\dot{\gamma}^2$, whereas $\{\mathbf{S}^2\} = 2\dot{\gamma}^2$, hence $R = 1$, and $D = 0$.

2.2.3. Non-uniform shear flow : Couette flow

We now consider the Couette flow of a Newtonian fluid between two cylinders with radius R_1 and $R_2 > R_1$. This flow is of particular interest because it is a shear flow having a non-uniform (space-dependent) shear rate. In a Couette flow, the fluid is submitted to a rotation induced by the movement of the inner cylinder at velocity ω_1. The velocity field in the polar basis $(\mathbf{e}_r, \mathbf{e}_\theta)$ corresponding to the polar coordinates (r, θ), is given as

$$v_r = 0, \qquad v_\theta = A\left(\frac{1}{r} - \frac{r}{R_2^2}\right), \tag{13}$$

where $A = \omega_1 R_1^2 R_2^2/(R_1^2 - R_2^2)$. Since there is no radial component of velocity, the particle trajectories are circles. From the velocity field, we can deduce the shear stress components and the vorticity tensor again expressed in the polar basis,

$$\mathbf{S} = \begin{bmatrix} 0 & -A/r^2 \\ -A/r^2 & 0 \end{bmatrix}, \quad \mathbf{W} = \begin{bmatrix} 0 & -A/R_2^2 \\ A/R_2^2 & 0 \end{bmatrix}. \tag{14}$$

It is interesting to note that the shear flow rate here depends on the radius r. The angle ϕ between the second eigenvector of $\mathbf{S}$ and the non-inertial polar basis is found to be $-\pi/4$, in agreement with the result for the uniform shear flow. This property holds whether the shear rate is uniform or not.

We know from the above arguments that the eigenvectors of $\mathbf{S}$ in a Couette flow have a fixed direction with respect to the polar basis $(\mathbf{e}_r, \mathbf{e}_\theta)$. From this, we deduce that from the point of view of an observer in an inertial reference frame the eigenvectors of $\mathbf{S}$ are rotating at the angular velocity v_θ/r. Therefore, the rate of rotation of the principal directions of $\mathbf{S}$, again expressed in the polar basis, is given by

$$\mathbf{\Omega} = \begin{bmatrix} 0 & A\left(\frac{1}{r^2} - \frac{1}{R_2^2}\right) \\ -A\left(\frac{1}{r^2} - \frac{1}{R_2^2}\right) & 0 \end{bmatrix}. \tag{15}$$

This simple example proves that the angular velocity $\mathbf{\Omega}$ can be non zero in flow regions characterized by a space-dependent shear rate. The case of the Couette flow is particularly illustrative in the discussion of MFI. From equations (15) and (14), it is found that the Euclidean objective vorticity tensor in a Couette flow is

$$\overline{\mathbf{W}} = \begin{bmatrix} 0 & -A/r^2 \\ A/r^2 & 0 \end{bmatrix}. \tag{16}$$

Hence, $\{\overline{\mathbf{W}}^2\} = \{\mathbf{S}^2\}$, which implies that $D = 0$. A Couette flow is a shear flow, and identified as such by the flow classifier D. Note that if $\{\mathbf{W}^2\}$ were to be used instead of $\{\overline{\mathbf{W}}^2\}$ in Eq. (9) the flow classifier D would not

be equal to zero, and the Couette flow would be misinterpreted as not being a shear flow.

From the above arguments, we can infer different flow patterns in which the angular velocity $\mathbf{\Omega}$ is likely to be non-zero. The first situation is the transition between regions having distinct uniform kinematics. For instance, in a region of transition between uniform extension and uniform shear, the angle ϕ ranges from $-\pi/2$ to $-\pi/4$. This will induce an anti-clockwise angular velocity $\mathbf{\Omega}$. The second situation is a shear flow including rotation, as illustrated by the Couette flow in which $\mathbf{\Omega}$ is clearly non-zero. More genererally, it is expected that flows implying significant rotation and (or) streamline curvature, such as flows in curved ducts for instance, should generate non-zero angular velocity of the principal directions of $\mathbf{S}$.

Finally, the special instance of rigid body motion (translation or rotation) should be mentioned. For rigid body motion, the principal directions of tensor $\mathbf{S}$ are not defined and we can arbitrarily force $\mathbf{\Omega}$ to be zero. As the flow approaches rigid body rotation, $\{\mathbf{S}^2\} \to 0$, hence $R \to \infty$ and $D \to -1$. For rigid body translation, both $\mathbf{S}$ and $\overline{\mathbf{W}}$ are zero, hence the parameter R is undetermined.

2.3. General method for complex two-dimensional flows

In complex flows the angular velocity $\mathbf{\Omega}$ must be evaluated numerically. Essentially, two methods exist to compute $\mathbf{\Omega}$. The first method requires to solve the tensorial equation (6). Since the evaluation of the eigenvectors is required, this direct approach is numerically costly and cumbersome, even for two-dimensional flows. This method can also cause troubles in the orientation of the eigenvectors since the eigenvector basis can be arbitrarily rotated of $\pm\pi$. In flows having strong streamline curvature (for instance the flow in a U-duct), it could generate erroneous values of $\mathbf{\Omega}$.

The second method was proposed by Gatski and Jongen, 2000 for two-dimensional flows. In 2D-flows the eigenvalues of $\mathbf{\Omega}$ are $\alpha_1 = -\alpha_2 = \sqrt{\{\mathbf{S^2}\}/2}$, with $\{\mathbf{S^2}\}$ the trace of $\mathbf{S^2}$. The angular velocity $\mathbf{\Omega}$ can be interpreted as the material derivative of the angle ϕ between the eigenvector basis and the fixed inertial basis, i. e.

$$\mathbf{\Omega} = \begin{bmatrix} 0 & -\dfrac{\mathrm{D}\phi}{\mathrm{D}t} \\ \dfrac{\mathrm{D}\phi}{\mathrm{D}t} & 0 \end{bmatrix}. \tag{17}$$

The material derivative of ϕ is given by (see Gatski and Jongen, 2000 for details)

$$\frac{\mathrm{D}\phi}{\mathrm{D}t} = \frac{1}{\{S^2\}}\left[S_{11}\frac{\mathrm{D}S_{12}}{\mathrm{D}t} - S_{12}\frac{\mathrm{D}S_{11}}{\mathrm{D}t}\right]. \tag{18}$$

In this study we used both methods and found that they provided the same results in the flows considered herein. The second method is numerically more efficient since it does not need any algorithm to compute the eigenvectors.

3. Kinematic results

We consider in this section the two-dimensional stream of a Newtonian viscous fluid past a circular cylinder of unit radius $A = 1$. The computational domain (Fig. 1) extends 15 cylinder diameters upstream, 30 diameters downstream, and 15 diameters on each side of the cylinder. The numerical results presented here are obtained from solutions of the Navier-Stokes equations written in general orthogonal coordinates (Pope, 1978)and using a finite volume discretization. These equations use physical orthogonal coordinates and physical contravariant velocities. The method is second-order accurate in space using a staggered grid, with the pressure at the center of the control volumes and the velocities at the center of the faces. The orthogonal grid was generated from the streamlines and lines of equal potential of the inviscid flow past the cylinder. This results in the 200×100 body-fitted structured grid presented in Fig. 1. For the advection terms a quadratic upstream interpolation scheme (QUICK) was used, whereas a centered difference scheme was employed for diffusion. The time discretization is semi-implicit resulting in a Poisson equation for the pressure (see Mompean and Deville, 1997 for details). Full details about the numerical procedure can be found in Thais et al., 2002.

On the cylinder's surface, non-slip impermeable boundary conditions are used. At the entrance of the flow domain, a uniform unit velocity field $U_0 = 1$ in the horizontal direction x is imposed. At the far-field outlet of the flow domain a zero pressure boundary condition is imposed. In the spanwise direction z, symmetry boundary conditions are imposed. For the present simulation, the Reynolds number $R_e = 2AU_0/\nu$ was set to 20, which is well below the admitted value for the primary 2D-instability (Williamson, 1996). Figure 1 displays contour lines of the stream function in the near wake of the cylinder. For $R_e = 20$, the flow is confirmed to be steady and symmetric with respect to $z = 0$, with the appearance of two recirculation vortices. The reattachment length L_A may be defined as the distance along the x axis, measured from the trailing edge of the cylinder, at

which the horizontal x velocity component changes sign from negative to positive. We find $L_A = 1.9$ in fairly good agreement with data from other sources (Braza et al., 1986).

The contours of the $12-$component of the angular velocity $\mathbf{\Omega}$, made dimensionless with $2A/U_0$, are presented in Fig .2. The field is anti-symmetric with respect to the axis $z = 0$, we shall comment the results for the upper part of the flow domain $z \geq 0$. The maximum of Ω_{21} is found in the shear layer near the cylinder at position $(x \simeq -0.5, z \simeq 1)$. We notice that the minimum of Ω_{21} (negative values) is in the immediate vicinity of the maximum. Also, Ω_{21} is significantly negative in a large region extending upstream and downstream of the location of the minimum.

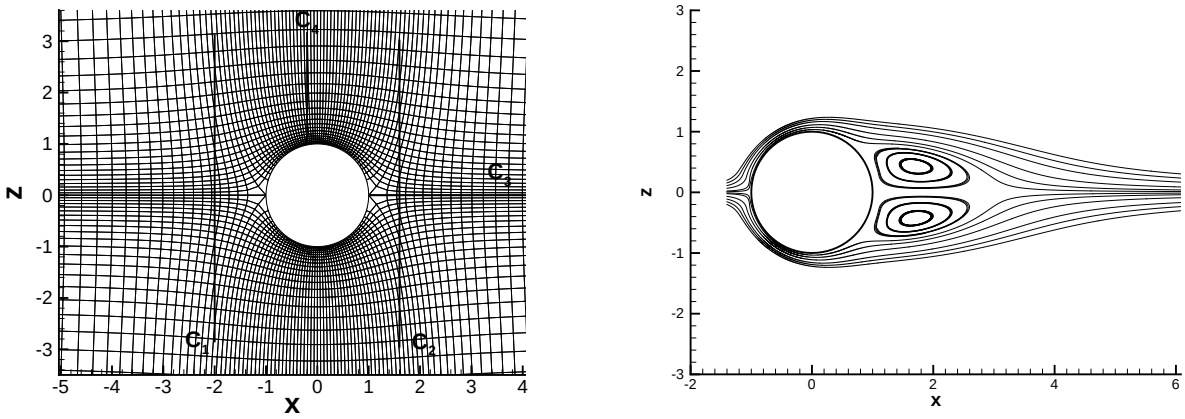

Figure 1: Zoom around circular cylinder of the body-fitted orthogonal mesh with 200×100 cells and definition of sections C_1, C_2, C_3, C_4 (left); Streamlines of steady flow past a circular cylinder, $R_e = 20$ (right).

Figure 2 shows the different regions of the flow past the cylinder using the classifier D. The field of D is symmetric with respect to $z = 0$, we shall comment the results for the upper part of the flow domain $z \geq 0$. Three limiting types of flow are identified. Two regions of extension, for which $D \simeq 1$, are observed near the symmetry axis $z = 0$. The first one is upstream of the cylinder and extends up to the "stagnation point"; the second region of extension starts downstream of the recirculation vortices $(z \geq 2)$.

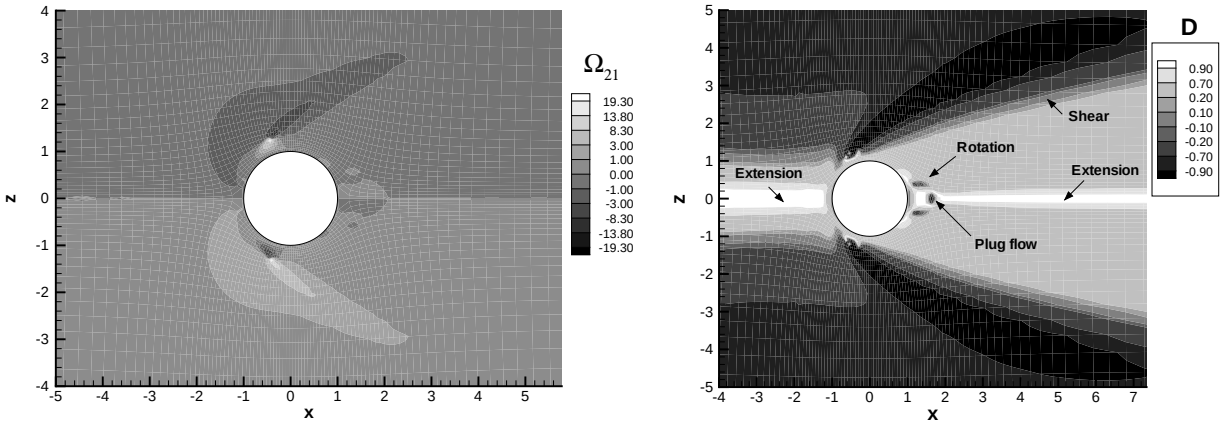

Figure 2: Angular velocity of the eigenvectors of the rate-of-deformation tensor (left) and contours of the objective D flow-type classifier (right) ; steady flow past a circular cylinder, $R_e = 20$.

As expected, a shear layer, for which $D \to 0$, is found to develop on each side of the cylinder. The shear layer zone starts from the point where Ω_{21} is maximum (see Fig. 2) and extends far downstream of the cylinder. It should be stressed that we do not identify a zone of uniform shear, for which $D = 0$. There are two regions where the values of D become negative and gets close to -1: (a) A spot around $(x = 1.2, z = 0.5)$ is observed corresponding to a rigid body rotation inside the recirculation vortex, (b) A spot around $(x = 1.8, z = 0)$

corresponding to a plug flow in-between the two recirculation vortices. Away from the cylinder, the flow is uniform, the principal directions of $\mathbf{S}$ are not defined and R cannot be evaluated. The value of D has been forced numerically towards -1 in this region.

Four sections C_1, C_2, C_3 and C_4 were chosen to examine the difference between $\mathbf{W}$ and the Euclidean objective vorticity tensor $\overline{\mathbf{W}}$, made dimensionless with $2A/U_0$ (see Fig. 1). Section C_1 is a cross-section located at $x = -2$. Section C_2 and C_3 are downstream of the cylinder. C_2 is located at $x = 1.6$ and crosses the two recirculation vortices, and C_3 is part of the symmetry axis $z = 0$. The fourth section, C_4, crosses the spot of maximum in Ω_{21}. Figure 3 displays the profiles of W_{21} and $\overline{W}_{21}$ along these sections.

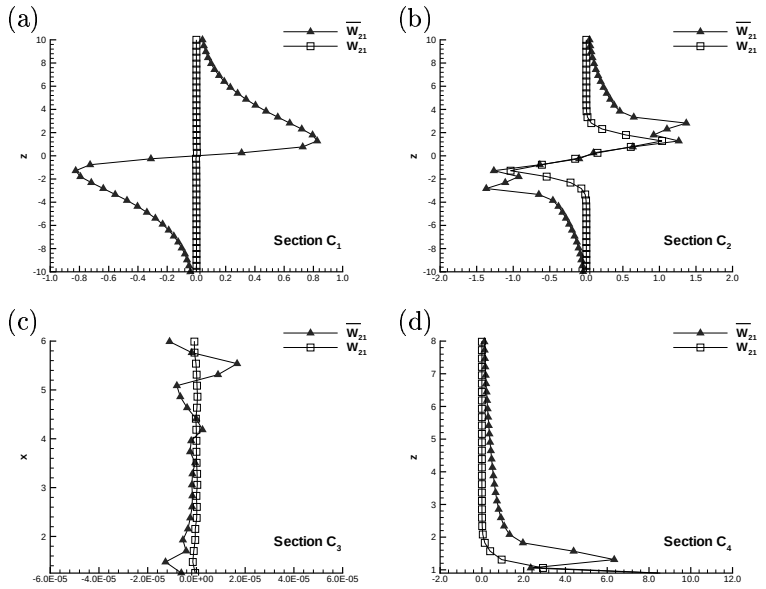

Figure 3: Profiles of $\overline{W}_{21}$ (▲) and W_{21} (□) along sections C_1, C_2, C_3 and C_4; steady flow past a circular cylinder, $R_e = 20$.

In section C_1 (Fig. 3a) the effects of angular velocity of the principal direction of $\mathbf{S}$ are most significant near $z = 2$. Away from the cylinder W_{21} and $\overline{W}_{21}$ tend towards the same value. In section C_2 (Fig. 3b), we note that in the recirculation vortices ($|z| \leq 1$) there is no difference between W_{21} and $\overline{W}_{21}$. The largest discrepancy is obtained around $z \simeq 3$ crossing the shear layer. In section C_3 (Fig. 3c), the magnitude of the two vorticity components are seen to be very small, of order 10^{-5}. This result is expected since section C_3 is along the symmetry axis $z = 0$. Section C_4 (Fig. 3d) exhibits the largest difference between W_{21} and $\overline{W}_{21}$ since it crosses the spot of maximum Ω_{21} near $z = 1.5$.

4. Consequences for algebraic stress models

The differences between the non-objective vorticity tensor $\mathbf{W}$ and the Euclidean objective vorticity tensor $\overline{\mathbf{W}}$ must induce some consequences in algebraic constitutive laws which include one or the other of these two tensors. In this section, the consequences of taking into account or neglecting MFI are quantified for a simple algebraic stress model applied to the flow past a circular cylinder.

4.1. Algebraic stress model

The derivation of algebraic stress models usually involves polynomial expansions of a traceless symmetric stress tensor. This technique was first proposed by Pope, 1975 for the anisotropy tensor in the framework of turbulence closure. A similar procedure can be used for modelling extra-stresses of viscoelastic liquids. In this context, denoting by $\boldsymbol{\tau}$ the polymeric part of the extra-stress tensor, a traceless symmetric extra-stress tensor is defined as

$$\boldsymbol{\Gamma} = \boldsymbol{\tau} - \frac{1}{3}\{\boldsymbol{\tau}\}\mathbf{I} \tag{19}$$

For two-dimensional (2-D) flows it is expanded according to

$$\mathbf{\Gamma} = \sum_{n=1}^{3} \beta_n \mathbf{T}^{(n)}, \tag{20}$$

where the three-term tensor base $(\mathbf{T}^{(1)}, \mathbf{T}^{(2)}, \mathbf{T}^{(3)})$ must include symmetric traceless tensors, and where the coefficients β_n are scalar functions. A non-objective algebraic stress model for 2-D flows was derived by Mompean et al., 1998 which uses

$$\mathbf{T}^{(1)} = \mathbf{S}, \quad \mathbf{T}^{(2)} = \mathbf{SW} - \mathbf{WS}, \quad \mathbf{T}^{(3)} = \mathbf{S}^2 - \frac{1}{3}\{\mathbf{S}^2\}\mathbf{I} \tag{21}$$

as the tensor base. A similar Euclidean objective algebraic stress model was later proposed by Mompean et al., 2003 in which the second base tensor $\mathbf{T}^{(2)} = \mathbf{S}\overline{\mathbf{W}} - \overline{\mathbf{W}}\mathbf{S}$, i.e. the non-objective vorticity tensor $\mathbf{W}$ was replaced by the Euclidean objective vorticity tensor $\overline{\mathbf{W}}$. In both the afore mentioned models the scalar coefficients β_n were calculated as functions of the scalar invariants of $\mathbf{\Gamma}$, $\mathbf{S}$ and $\mathbf{W}$ (or $\overline{\mathbf{W}}$).

For the purpose of the present study, we shall use a simpler model (Debbaut, 2003) which assumes constant coefficients given by $\beta_1 = 2\eta$, $\beta_2 = 2\eta\lambda$, $\beta_3 = 4\eta\lambda$, where η is the polymeric viscosity and λ the relaxation time of the viscoelastic fluid. These coefficients were found by requiring the algebraic model to reproduce the uniform shear stress properties of the Oldroyd-B model. The non-objective version of the present model under consideration will therefore assume a traceless stress

$$\mathbf{\Gamma} = 2\eta\,\mathbf{S} + 2\eta\lambda\,(\mathbf{SW} - \mathbf{WS}) + 4\eta\lambda\left(\mathbf{S}^2 - \frac{1}{3}\{\mathbf{S}^2\}\mathbf{I}\right) \tag{22}$$

In this expression we can identify three contributions. The first term $2\eta\,\mathbf{S}$ is a purely *viscous contribution*; the second one $2\eta\lambda\,(\mathbf{SW} - \mathbf{WS})$ includes the vorticity tensor and will be named hereafter *rotational contribution*; and the third one $4\eta\lambda\left(\mathbf{S}^2 - \frac{1}{3}\{\mathbf{S}^2\}\mathbf{I}\right)$ will be named the *quadratic contribution.*

The Euclidean objective version of the same model is simply obtained upon replacing $\mathbf{W}$ by $\overline{\mathbf{W}}$ in Eq. (22) which gives

$$\overline{\mathbf{\Gamma}} = 2\eta\,\mathbf{S} + 2\eta\lambda\left(\mathbf{S}\overline{\mathbf{W}} - \overline{\mathbf{W}}\mathbf{S}\right) + 4\eta\lambda\left(\mathbf{S}^2 - \frac{1}{3}\{\mathbf{S}^2\}\mathbf{I}\right) \tag{23}$$

The difference between the Euclidean objective and non-objective laws rests on the sole *rotational contribution.* For the present study, a given flow kinematics was used to evaluate the extra stresses in Eq. (22) and (23), there is no coupling between the constitutive laws and the flow dynamics.

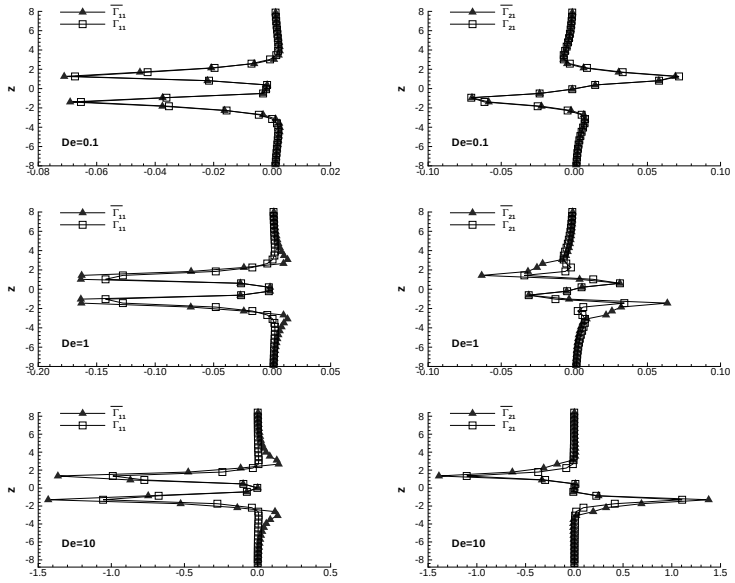

Figure 4: Cross profiles along section C_2 of: objective (▲) and non-objective (□) extra-stresses for 3 Deborah numbers $D_e = 0.1$ (top), $D_e = 1$ (middle), $D_e = 10$ (bottom); $11-$component (left), $21-$component (right); steady flow past a circular cylinder, $R_e = 20$.

4.2. Results for the cylinder

Profiles of extra-stresses are plotted along section C_2 in Fig. 4, and along section C_4 in Fig. 5. Section C_2 is downstream of the cylinder crossing the two recirculation vortices. Section C_4 crosses the region where Ω_{21} is maximum (see Fig. 2). The results will be presented for 3 increasing Deborah numbers $De = \lambda U_0/2A$, based on the downstream average velocity U_0 and the cylinder diameter $2\,A$, namely $De = 0.1$, 1 and 10 from top to bottom in Fig. 4 and 5.

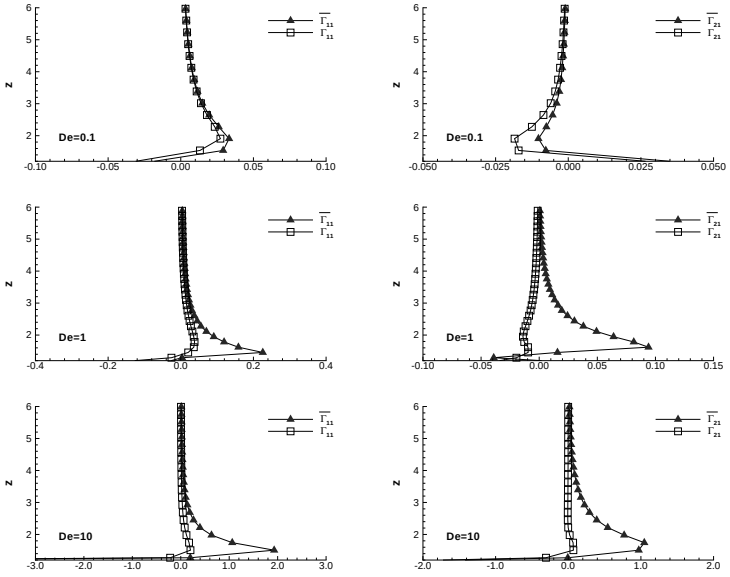

Figure 5: Cross profiles along section C_4 of: objective (▲) and non-objective (□) extra-stresses for 3 Deborah numbers $D_e = 0.1$ (top), $D_e = 1$ (middle), $D_e = 10$ (bottom); $11-$component (left), $21-$component (right); steady flow past a circular cylinder, $R_e = 20$.

We observe in these figures that the role of MFI increases with increasing Deborah number, yet the discrepancy between the Euclidean objective and non-objective constitutive laws remains small to moderate for the section (C_2). A noticeable result seen in Fig. 4 is that there is no difference between the Euclidean objective and non-objective extra-stresses in the region crossing the recirculation vortices, irrespective of the Deborah number. For this section (C_2) the MFI could be reasonably ignored. In section C_4 (Fig. 5), the role of MFI is significantly more pronounced than observed in the previous section. In particular, it should be noticed that the Euclidean objective and non-objective extra-stresses can have a difference of one order of magnitude close to the region where Ω_{21} is maximum ($z = 1.5$).

5. Conclusions

This paper presents a methodology to identify regions of a flow field where the principle of material frame-indifference (MFI) should be taken into account or could be reasonably discarded. The method consists of computing an Euclidean objective vorticity tensor $\overline{\mathbf{W}}$ defined as the difference between the usual vorticity tensor $\mathbf{W}$ and the angular velocity $\mathbf{\Omega}$ of the eigenvectors of the rate-of-deformation tensor. The role of MFI is likely to appear in regions of a flow where $\mathbf{\Omega}$ is significant in magnitude with respect to $\mathbf{W}$. This method was applied to a uniform stream past a circular cylinder. This configuration exhibits complex flow kinematics, including shear layers, extension and recirculation zones.

The first result of this study is that $\mathbf{\Omega}$ is negligible in regions of the flow characterized by uniform shear or extension and in the recirculation zones. In contrast, obtaining significant values of $\mathbf{\Omega}$ requires a transition between regions having different kinematics **and** a significant velocity magnitude. This situation was observed in the shear layer of the flow past a cylinder (section C_4). The latter result is in agreement with Eq. (18), in which it can be seen that the angular velocity $\mathbf{\Omega}$ is proportional to deformation rates and to the velocity components appearing in the material derivatives. The second important result is the influence of this kinematic result upon MFI. This was checked upon comparing the stresses obtained by use of given Euclidean objective (Eq. 23) and non-objective (Eq. 22) constitutive laws. As expected the overall effect of MFI increases with the Deborah number. Quantitatively, for $De = 0.1$ in all flow configurations we found small departures between

Euclidean objective and non-objective stresses. For $De = 10$ in the most critical region, the Euclidean objective and non-objective stresses can differ by one order of magnitude (see bottom of Fig. 5). On the other hand, regions where the magnitude of $\mathbf{\Omega}$ is small will in any event never be sensitive to MFI. In such regions MFI can be safely ignored. When interpreting these results it should be borne in mind that there is no dynamical coupling between the flow and the constitutive laws. This should have little impact at small Deborah numbers, but future work is necessary to check the influence of MFI when coupling Euclidean objective stress models at high Deborah numbers.

6. Acknowledgements

The authors acknowledge the French 'Ministère de la recherche et de l'industrie' for the financial support of the project Eureka Σ!2799, ScaFTen (Scalar For Tensor) and wish to thank the participating companies Michelin and Polyflow s.a./Fluent Benelux.

7. References

Astarita, G., 1979, Objective and generally applicable criteria for flow classification, "J. Non-Newtonian Fluid Mech.", Vol. 6, pp. 69–76.

Braza, M., Chassaing, P., and Minh, H. H., 1986, Numerical study and physical analysis of the pressure and velocity fields in the near wake of a circular cylinder, "J. Fluid Mech.", Vol. 165, pp. 79–130.

Debbaut, B., 2003, Private communication, Vol. .

Drouot, R., 1976, Définition d'un transport associé à un modèle de fluide du deuxième ordre. Comparaison de diverses lois de comportement., "C. R. Acad. Sc. Paris, Série A", Vol. 282, pp. 923–926.

Gatski, T. B. and Jongen, T., 2000, Nonlinear eddy viscosity and algebraic stress models for solving complex turbulent flows, "Progress in Aerospace Sciences", Vol. 36, pp. 655–682.

Joseph, D. D., 1990, "Fluid Dynamics of Viscoelastic Liquids", Applied Mathematical Sciences, Springer-Verlag, New-York.

Liu, I. S., 2004, On Euclidean objectivity and the principle of material frame-indifference, "Continuum Mech. Thermodyn.", Vol. 16, pp. 177–183.

Mompean, G. and Deville, M., 1997, Unsteady finite volume simulation of Oldroyd-B fluid through a three-dimensional planar contraction, "Journal of Non-Newtonian Fluid Mechanics", Vol. 72, pp. 253–279.

Mompean, G., Jongen, T., Gatski, T., and Deville, M., 1998, On algebraic extra-stress models for the simulation of viscoelastic flows, "Journal of Non-Newtonian Fluid Mechanics", Vol. 79, pp. 261–281.

Mompean, G., Thompson, R. L., and Souza Mendes, P. R., 2003, A general transformation procedure for differential viscoelastic models, "J. Non-Newtonian Fluid Mech.", Vol. 111, pp. 151–174.

Murdoch, A. I., 2003, Objectivity in classical continuum physics: a rationale for discarding the 'principle of invariance under superposed rigid body motions' in favour of purely objective considerations, "Continuum Mech. Thermodyn.", Vol. 15, pp. 309–320.

Oldroyd, J. G., 1950, On the formulation of rheological equations of state, "Proc. Roy. Soc. London A", Vol. 200, pp. 523–541.

Pope, S., 1975, A more general effective-viscosity hypothesis, "J. Fluid Mech.", Vol. 72, pp. 331–340.

Pope, S. B., 1978, The calculation of turbulent recirculating flows in general orthogonal coordinates, "J. Comp Phys.", Vol. 26, pp. 197–217.

Ristorcelli, J. R., Lumley, J. L., and Abid, R., 1995, A rapid-pressure correlation representation consistent with the Taylor-Proudman theorem and materially frame-indifferent in the 2-D limit, "J. Fluid Mech.", Vol. 292, pp. 111–152.

Rumsey, C. L., Gatski, T. B., and Morrison, J. H., 2000, Turbulence model predictions of strongly curved flow in a U-duct, "AIAA Journal", Vol. 38, No. 8, pp. 1394–1402.

Speziale, C. G., 1998, A review of material frame-indiference in mechanics, "App Mech Rev", Vol. 51, No. 8, pp. 489–504.

Thais, L., Mompean, G., and Naji, H., 2002, Computation of flow past a circular cylinder using general orthogonal coordinates, Mang, H., Rammerstorfer, F., and Eberhardsteiner, J., editors, "Proc. of the Fifth World Congress on Computational Mechanics (WCCM V), Vienna, Austria".

Truesdell, C. and Noll, W., 1965, "The non-linear field theories of mechanics", In: Flugge, S. (ed) Handbuch der Physik, Vol. III/3, Springer-Verlag Berlin Heidelberg.

Williamson, C. H. K., 1996, Vortex dynamics in the cylinder wake, "Annu. Rev. Fluid Mech.", Vol. 28, pp. 477–539.